UV radiation in Ar-O_2, N_2-O_2 and Ar-O_2-N_2 microwave discharges and post-discharges

K. Kutasi[1], V. Guerra[2], P. Sá[2,3], J. Loureiro[2]

[1]*Research Institute for Solid State Physics and Optics of the Hungarian Academy of Sciences, POB 49, H-1525 Budapest, Hungary*
[2]*Instituto de Plasmas e Fusão Nuclear, Instituto Superior Técnico, 1049-001 Lisboa, Portugal*
[3]*Departamento de Engenharia Física, Faculdade de Engenharia da Universidade do Porto, 4200-465 Porto, Portugal*

This work presents a theoretical investigation on the production of active species in low-pressure Ar-O_2 and Ar-O_2-N_2 microwave discharges, and the evolution of the species densities along the afterglow. Special attention is given to the UV emitting species, such as Ar(4s) excited states, and NO(A) and NO(B) molecules. It is shown that, for the conditions of the present study, the active species are efficiently produced in the discharge, however their lifetime in the afterglow is limited. We have shown that the Ar(4s) excited states depopulate during 10^{-4} s afterglow time in pure Ar, and the depopulation becomes faster with O_2 addition. In what concerns the NO(A) and NO(B) molecules, their densities increase with the N_2 addition to the Ar-2%O_2 mixture. The NO(A) density has found to be maximum in the discharge in 98%N2-2%O2 mixture, as well as the N and O atoms densities.

1. Introduction

Post-discharge plasmas have a wide range of applications, such as metal surface cleaning, medical sterilization, etching and grafting, thin film synthesis, etc. The post-discharges of Ar-O_2 and N_2-O_2 flowing microwave discharges have been found to be very efficient in the bacterial spore removal [1-3]. Kylián et al. [4] have studied a low pressure Ar-O_2-N_2 ICP discharge in order to evaluate its properties in terms of sterilization. They have demonstrated that the application of Ar-O_2-N_2 ternary mixture offers the possibility to combine the advantageous properties of the above-mentioned binary mixtures. The main sterilizing agents in Ar-O_2 and N_2-O_2 plasmas it is believed [1,3,5] to be the O atoms and UV photons. The aim of the present study is to investigate the evolution of the UV radiation when changing from binary mixtures to the ternary mixture.

2. System set-up

The post-discharge system used in our investigations is similar to the one used in the sterilization experiments by the Montréal group [6]. Here the surface wave discharge is generated in a R= 5 mm silica tube with 2450 MHz frequency field. The discharge and the reactor are linked through two tubes of different diameters, whereas the first tube, right after the discharge zone, has the same diameter as the discharge tube, the second tube is widened to 2.6 cm relatively to the discharge tube. Herein we focus our attention on the discharge and early afterglow region and assume that the radius of the tube where the early-afterglow develops has the same size as the discharge tube. Our calculations are conducted in Ar-O_2, N_2-O_2 and Ar-O_2-N_2 mixtures, respectively, for different mixture compositions at 2 Torr pressure.

3. Model

The system is described with two different models valid for the discharge and early afterglow region, and for the late afterglow present in the large reactor, respectively. The species densities in the discharge region are calculated by solving the homogeneous electron Boltzmann equation, coupled together with the rate balance equations of different species. The concentrations obtained for the steady-state discharge are used as initial values to the early afterglow taking place in the tube connecting the discharge to the main reactor, where the same system of equations is solved in time under zero electric filed [7,8]. The evolution of the species densities in the post-discharge reactor is followed with a 3-D hydrodynamic model [9].

In the model of the Ar-O_2 system the species taken into account are: Ar($^1S_0$,$^3P_2$,$^3P_1$,$^3P_0$,$^1P_1$), O_2($X^3\Sigma_g^-$,v), O_2($a^1\Delta_g$, $b^1\Sigma_g^+$), O(^3P,^1D), O_3, Ar^+, Ar_2^+, O_2^+, O^+, O^-; while in the Ar-N_2-O_2 system to the above listed species the N containing species are still added, i.e.: N_2(X,v), N(^4S,^2D,^2P),

N_2(A,B,B',C,a',a,w), NO_2(X, A), NO(X, A, B), N_2^+(X, B), N_4^+ and NO^+. In the hydrodynamic model of the late-afterglow we neglect some of the excited species and all the ions, since due to deactivation and recombination their densities become negligible in the reactor. The set of gas phase reactions describing the kinetics of species as considered in the post-discharge chamber and discharge region for the nitrogen and oxygen containing species has been presented in [8,10] and the references therein. A set of reactions for the Ar, Ar-N_2 and Ar-O_2 mixtures can be found in [12-14]. The surface reactions involving the N and O atoms have been discussed in details in [11].

4. Results

The UV radiation in Ar-O_2 discharge is due to the Ar($^3P_1$,$^1P_1$) resonant states, while in N_2-O_2 mostly to the NO(A) and NO(B) molecules.

As a first step we investigate the densities of Ar($^3P_1$,$^1P_1$) resonant states in Ar-O_2 mixture, and the evolution of these densities in the early-afterglow region. Figure 1 shows the calculated Ar($^3P_1$,$^1P_1$) densities as a function of the early-afterglow time (flight-time of species in the afterglow, where t=0 means the end of the discharge) in Ar and in Ar-O_2 mixture with 1% and 2%O_2 addition. The calculations show that the in pure Ar the resonant states depopulate within 0.1 ms in the early-afterglow. Moreover, with oxygen addition the depopulation occurs faster. This is a consequence of to the quenching of Ar 4*s* ($^3P_2$,$^3P_1$,$^3P_0$,$^1P_1$) states by O_2 through reaction Ar(4s)+O_2→Ar($^1S_0$)+O(^{3}P) +O(^{3}P,^{1}D). The results here obtained suggest that in the late afterglow present in a large reactor no UV emission can be expected from the Ar($^3P_1$,$^1P_1$) states.

Figure 2 shows the evolution of oxygen O(^{3}P) and O(^{1}D) atoms in the afterglow. We can notice the steep increase of the O atoms upon oxygen addition into an argon discharge, and that oxygen is strongly dissociated by electron impact and by the Ar metastables (above mentioned reaction), the dissociation degree being in the range of 25-50%. Similar results have also been obtained experimentally by Mozetič et al. [15] where the density of O(^{3}P) ground state atoms has been determined both by NO titration and catalytic probe methods.

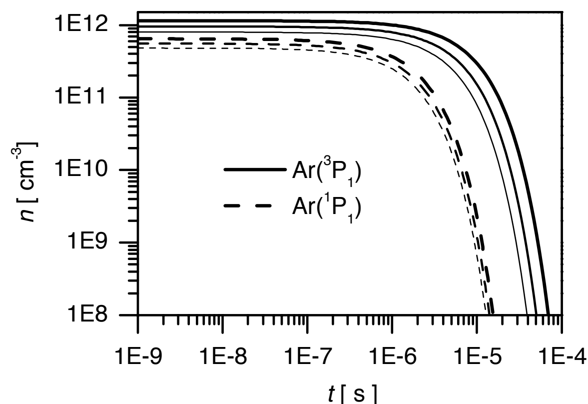

Figure 1. Time evolution of the Ar atoms resonant states densities along the early afterglow (*t*=0 means the end of the discharge) in Ar (thick line) and in Ar-O_2 mixture with 1% and 2%O_2 addition (thinnest line).

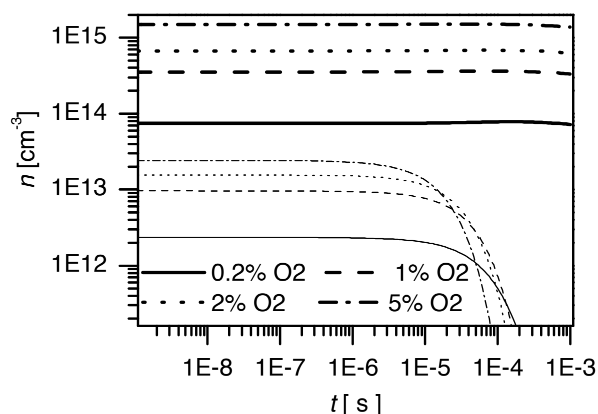

Figure 2. Time evolution of O(^{3}P) (thick lines) and O(^{1}D) (thin lines) atoms densities along the early afterglow in Ar-O_2 mixtures with different O_2 addition.

As a second step N_2 (from 0.2 to 98%) was added into the Ar-O_2 mixture while the O_2 percentage in the mixture was kept constant at 2%. Figure 3 a) and b) shows the evolution of NO(A) and NO(B) densities in the early-afterglow. In the discharge the NO(A) molecules are mainly created from the collision of NO(X) with N_2(A) metastable molecules: NO(X)+N_2(A)→NO(A)+N_2(X), while NO(B) molecules are created through the three body re-association of N and O atoms: N+O+M →NO(B)+M [6]. Consequently, in the discharge NO(A) is always significantly more populated than NO(B) and the time evolution of these two states is quite different in the early afterglow, up to times 10^{-4}-10^{-3} s, as illustrated in Figure 3.

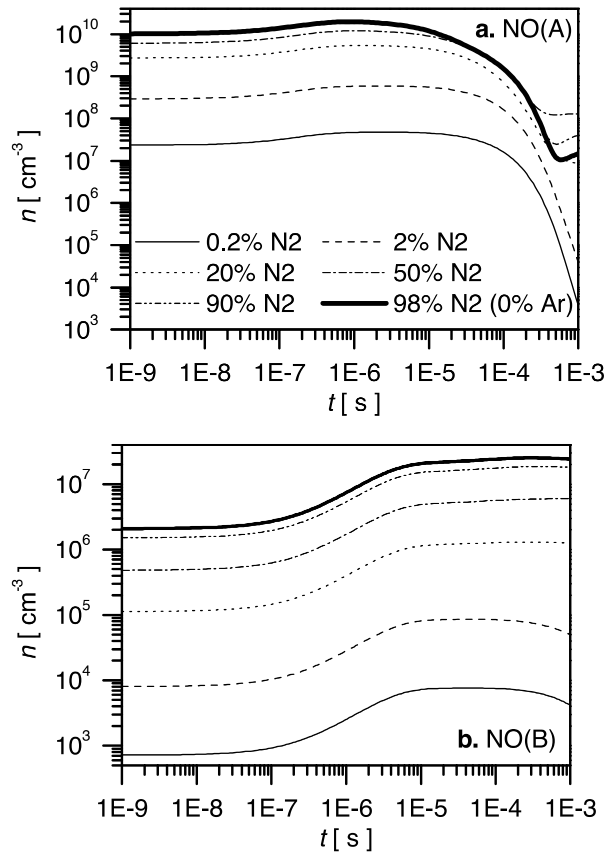

Figure 3. Time evolution of (a) NO(A) and (b) NO(B) molecules densities along the early afterglow in Ar-O_2-N_2 mixtures with different N_2% addition into Ar-2%O_2.

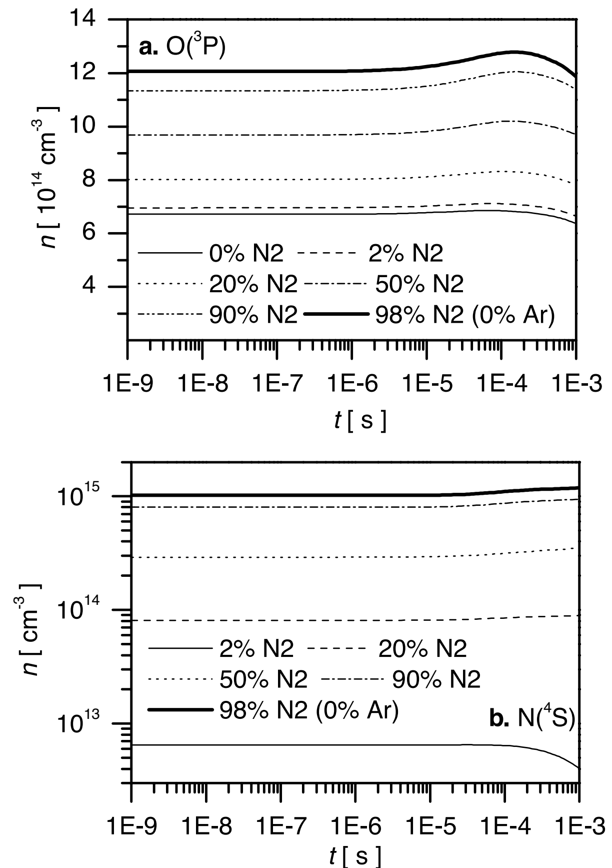

Figure 4. Time evolution of (a) O(^{3}P) and (b) N(^{4}S) atoms densities along the early afterglow in Ar-O_2-N_2 mixtures with different N_2% addition into Ar-2%O_2.

The calculations show that the highest NO(A) density is obtained in the 98%N_2-2%O_2 mixture. However at around 0.1 ms in the afterglow this density decreases below the one obtained in mixtures of 50% and 90% N_2. From this position in the afterglow NO(A) molecules are dominantly created through the three body re-association of N and O atoms, similarly to the case of NO(B) molecules [6]. Therefore, the densities of NO(A) and NO(B) UV emitting molecules in the afterglow are controlled by the N and O atoms densities and, for longer afterglow times, have a rather similar evolution. Notice that N_2 concentrations and higher strongly favour the presence of NO(A) molecules in the late afterglow.

Figure 4 a) and b) shows the O and N atoms densities, respectively, along the ealy-afterglow for different N_2 addition to the Ar-2%O_2 mixture. The results show that the atomic species N and O do not change significantly in the early afterglow, and both increase with N_2 addition into the mixture.

As the oxygen concentration is fixed to 2%, the rate of O atom production in the discharge by electron impact is nearly constant when nitrogen is added into the mixture. Near pure Argon, an additional atomic oxygen source is dissociation due to collisions with the Ar(4s) states, as referred above. Evidently, this mechanism looses importance for higher N_2 concentrations in the mixture. However, the disappearance of this process is compensated by the raise in the contribution of other dissociation mechanisms, which become influential for significant nitrogen percentages, such as O_2 dissociation in collisions with N_2 excited molecules, N_2(B, a, a')+O_2→N_2+O+O. The dominant reaction is the one involving N_2(B) molecules. As an outcome, higher O atom concentrations are observed for higher nitrogen percentages in the mixture, as it can be seen in figure 4 a).

In turn, the N atom density increase in the discharge with N_2 content revealed by figure 4 b) is basically justified by the direct dissociation of N_2 molecules, the density of the latter course increasing. Nitrogen molecules are mostly dissociated by direct electron impact and, to a smaller extent, by collisions between N_2(A)

molecules and vibrationally excited molecules. Reaction $N_2(X,v\geq13)+O\rightarrow NO+N$, although exhibiting a very absolute high rate, does not contribute to the creation of N atoms as it does not prevail over the reverse process $N+NO\rightarrow N2(X,v\approx3)+O$ [16]. Another relevant dissociation mechanism is the destruction of NO via $N_2(a')+NO\rightarrow N_2+N+O$.

The present investigation casts light into the elementary processes responsible for the creation of the UV emitting species in the afterglow of the Ar-O_2-N_2 plasmas used in plasma sterilization reactors. It is shown the kinetics of these species is strongly coupled with the atomic species N and O. For the moment we have addressed the characterization of the discharge and early afterglow. The study of the species distribution in an actual reactor will be performed in the near future.

Acknowledgement

The work has been supported by the Hungarian Science Foundation OTKA, through project F-67556, Bolyai Fellowship of K.K. and Portuguese Science Foundation FCT.

3. References

[1] S. Moreau, M. Moisan, M. Tabrizian, J. Barbeau J. Peltier, A. Ricard, J. Appl. Phys. **88** (2000) 1166.
[2] S. Villeger, S. Cousty, A. Ricard, M. Sixou, J. Phys. D: Appl. Phys. **36** (2003) L60.
[3] M.K. Boudam, B. Saoudi, M. Moisan, A. Ricard, J. Phys. D: Appl. Phys. **40** (2007) 1694.
[4] O. Kylián and F. Rossi, J. Phys. D: Appl. Phys., **42** (2009) 085207.
[5] N. Philip et al., IEEE Trans. Plasma Sci. **30** (2002) 1429.
[6] K. Kutasi, B. Saoudi, C. D. Pintassilgo, J. Loureiro, M. Moisan, Plasma Processes and Polymers **5** (2008) 840.
[7] V. Guerra, J. Loureiro Plasma Sources Sci. Technol. **8** (1999) 110
[8] C.D. Pintassilgo, J. Loureiro, V. Guerra, J. Phys. D: Appl. Phys. **38** (2005) 417.
[9] K. Kutasi, C. D. Pintassilgo, J. Loureiro, 2nd Int. Workshop on Non-equilibrium Processes in Plasmas and Environmental Science, Journal of Physics: Conference Series 162 (2009) 012008
[10] K. Kutasi, C.D. Pintassilgo, J. Loureiro, P.J. Coelho, J. Phys. D: Appl. Phys. **40** (2007) 1990.
[11] K. Kutasi and J Loureiro, J. Phys. D: Appl. Phys. **40** (2007) 5612.
[12] C. M. Ferreira, J. Loureiro, A. Ricard, J. Appl. Phys. **57** (1985) 82.
[13] J. T. Gudmundsson and E. G. Thorsteinsson, Plasma Sources Sci. Technol. **16** (2007) 399; T. Sato and T.Makabe, J. Phys. D: Appl. Phys. **41** (2008) 035211.
[14] P. Sá and J. Loureiro, J. Phys. D: Appl. Phys. **30** (1997) 2320.
[15] M. Mozetič et al., J. Vac. Sci. Technol. A **21** (2003) 369.
[16] V. Guerra and J. Loureiro, Plasma Sources. Sci. Technol. **6** (1997) 373.